# Improving Mobile Internet Quality of Experience

Mallesham Dasari
Computer Science Department, Stony Brook University, Stony Brook, NY

## ABSTRACT

Mobile Internet applications have become predominant with the prolific increase in smartphone usage. Typically, these applications are Web browsing and video applications such as streaming and interactive telephony. The problem here is that the applications are influenced by a number of factors such as the network parameters, hardware performance and the inherent application complexity. This makes it hard to pinpoint and diagnose the problem, bringing new challenges in providing a good quality of experience (QoE) for these applications. To this end, we first conduct a systematic survey of existing literature that makes effort to improve the mobile Internet QoE. We then show the evidence for limitations of prior work in QoE optimizations in terms of network and device performance. Our contributions of this work are twofold. First, we propose a machine learning based QoE model that is hooked on top of WiFi access point or a cellular base station. The model learns the QoE of applications under diverse network conditions and help the network administrator in network resource provisioning according to the end-user QoE rather than traditional quality of serive (QoS) parameters. Second, we dig deep into the effect of underlying device performance to understand device side bottlenecks while providing unlimited network resources. This investigation brings a variety of strategies to content providers in placing the optimizations at mobile device or the network side which is especially important for the people of developing regions. Our experimental results shows that the behavior of these applications varies significantly from one another with respect to both network and hardware resources. We show the performance of these applications by selecting most popular applications such as YouTube for streaming, Skype for telephony and Google chrome for Web browsing.

## 1. INTRODUCTION

## 2. INTRODUCTION

Over the past decade, mobile video traffic has increased dramatically (from 50% in year 2011 to 60% in 2016 and is predicted to reach 78% by 2021) [24]. This is due to the proliferation of mobile video applications (such as Skype, FaceTime, Hangouts, YouTube, and Netflix etc). These applications can be categorized into video telephony (Skype, Hangouts, FaceTime), streaming (YouTube, Netflix), and upcoming virtual reality and augmented reality streaming (SPT [5], theBlu [6]). Users demand high Quality of Experience (QoE) while using these applications on wireless networks, such as WiFi and LTE. This poses a unique challenge for network administrators in enterprise environments, such as offices, university campuses and retail stores.

Guaranteeing best possible QoE is non-trivial because of several factors in video delivery path (such as network conditions at the client side and server side, client device, video compression standard, video application). While application content providers focus on improving the server-side network performance, video compression and application logic, enterprise network administrators seek to ensure that network resources are well provisioned and managed to provide good experience to multiple users of diverse applications. In this pursuit, network administrators can only rely on passive in-network measurements to *estimate* the exact user experience on the end-device. In this context, several prior works have developed a mapping between network Quality-of-Service (QoS) and end-user QoE for video applications [12, 11, 14], by using machine learning (ML) models and network features from PHY to TCP/UDP layers. ML models for QoE can be deployed at a number of vantage points in the network, such as access points, network controllers, cellular packet core.

In order to train any QoS to QoE model, one needs accurate ground-truth annotation of the QoE. To obtain this, prior work has leveraged application specific APIs such as Skype technical information [23] or YouTube API [11]; call duration [8]; or instrumented client-side libraries for video delivery platform [12]. While these solutions perform well for specific applications and providers, network administrators have to *deal with a plethora of video applications* and they *cannot control the application logic* for most applications. Nor does every application expose QoE metrics through APIs. Thus, to develop QoS to QoE models in the wild, network administrators need an application-independent approach to measure QoE. Note that application independence does not mean that modeling is application-agnostic, as a single QoE model cannot apply to all applications. Different applications exhibit diverse artefacts when quality deteriorates. For instance, streaming quality is impacted largely by buffering and stall ratio, whereas telephony quality is impacted by bit rate, frames per second, blocking and blurring in the video.

In this work, we propose a generic video telephony QoE model which does not rely on application support. Additionally, it is scalable to diverse content, devices and categories of video application. We take a similar approach as Jana *et al* [16], where we record the screen on the mobile device and estimate video quality. Different from previous works, we exploit video compression methods (Section 4) and identify four new metrics: *perceptual bitrate (PBR)*, *freeze ratio*, *length* and *number of video freezes* to measure the video QoE. We further demonstrate that our metrics are insensitive to the content of the video call and they only capture the *quality* of the video call (Section 6). We make a rigorous analysis of our model performance by conducting a large scale user-study of 800 video clips across 20 videos and more than 200 users. We conduct an extensive analysis on different types of users' devices and OS (Android vs. iOS), video content and motion.

We micro-benchmark our metrics under different network conditions to show that the metrics are agnostic to motion and content of the video. Further, we show that these met-

rics capture spatial and temporal artefacts of video experience. We then validate our metrics by mapping them to actual users' experience. To this end, we obtain Mean Opinion Score (MOS) from our user-study and apply ML models to map our metrics with users' MOS. We use `Adaboosted` decision trees in predicting the MOS scores, as we describe in Section 6.

In summary, our contributions are the following:

- We uncover limitations of existing work for QoE annotation of video telephony in enterprise networks (Section 3).
- We introduce new QoE metrics for video telephony that are content, application and device independent (Section 5).
- We micro-benchmark our metrics with the three most popular applications, i.e., Skype, FaceTime and Hangouts, and five different mobile devices (Section 5).
- We develop a model to map our QoE metrics to MOS and demonstrate a median 90% accuracy across applications and devices (Section 6).

## 3. MOTIVATION FOR SCALABLE QOE ANNOTATION

In this section, we describe the need for new QoE metrics for enterprise networks and the limitations of existing work.

**Lack of QoE information from applications**: While several works have motivated and addressed the problem of network-based QoE estimation [11], little attention has been paid to the problem of collecting the QoE ground-truth. Most works have relied on application-specific information. This approach is effective for QoE optimizations by content providers, as they only focus on a single application [12] or initial training of QoS to QoE model [11]. Nevertheless, administrators of access networks have to ensure good experience for a wide range of diverse applications being simultaneously used. Table 1 shows that not all popular video applications provide QoE information. Even for applications like Skype, availability of technical information depends on the version of the application and on the OS (e.g., no technical information for iOS).

| Application | Ground-truth |
|---|---|
| Skype | ✓*on some versions |
| Hangouts/Duo | × |
| FaceTime | × |
| YouTube/Netflix | ✓ |

Table 1: Availability of QoE ground-truth

To apply QoE estimation models in real networks, we need to remove the dependency of QoE metrics on application features, such as Skype technical information. One way to achieve this is to simply record the video as it plays on the mobile device and analyze this video for quality.

**Lack of scalable and reliable QoE measures:** Prior work on video quality evaluation leverages *subjective and/or objective* metrics. Subjective metrics are measured with MOS collected through user surveys. They capture absolute QoE but are tedious to conduct and to scale. QoE metrics need to scale to thousands of videos in order to train models that map QoS to QoE. Alternatively, objective metrics can be computed from the video. Objective metrics are further classified in two categories: reference and no-reference based. A reference-based metric uses both sent and received video, and compares the quality of sent vs. received frames. As it is challenging to retrieve and synchronize reference videos for telephony applications, no-reference based quality metrics are preferred. Jana *et al* [16] have proposed a no-reference metric for QoE estimation in Skype and Vtok. They record received videos for each of these mobile telephony applications and compute three no-reference metrics: *blocking, blurring* and *temporal variations*. Then, they combine these three metrics into one QoE metric by using MOS from subjective user study. Their study shows that blocking does not impact MOS of a video clip. While they show that their *blur* and *temporal variation* metrics correlate well with MOS, they do not evaluate these metrics over a wide range of clips. For example, one can wonder if *blur* is sensitive to the video content.

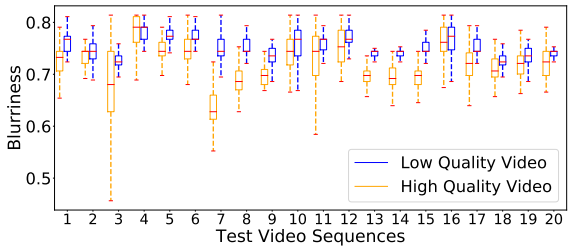


Figure 1: Blur detection using DCT coefficients [16, 17]. DCT coefficients fail to distinguish between high and low quality video due to content diversity.

We conduct similar experiments with Skype to evaluate blur metric of prior works. Our experimental setup is described in Section 5. To capture video blur, Jana *et al* [16] employ discrete cosine transform (DCT) coefficients [17] from the compressed data by computing the histogram of DCT coefficients thereby characterizing the image quality. The DCT coefficients are obtained in transform coding of video compression process, as described in Section 4. The assumption here is that blurred image has high-frequency coefficients close to zero. Hence, the method studies the distribution of zero coefficients instead of absolute pixel values. Although the method estimates out-of-focus blur accurately, it falls short in estimating realistic blur and sensitivity to noise. The authors also point out that the method is very sensitive to uniform background and images with high luminance components. In Fig. 1, we evaluate blur for 20 video sequences[1] using DCT metric. We have collected these videos in a representative manner to cover diverse content, different types of motion and we have downloaded them in Full HD resolution. The same 20 videos are converted to low quality by compressing and decreasing the resolution, to observe the difference of DCT metric between high and low quality videos.

We notice two aberrations of the DCT metric by Jana *et al* [16]: First, the metric is indeed content-specific i.e., although it produces high blur values for some low quality videos, it also shows high blur values for some high quality videos. For instance, videos 2 and 4 contain mostly over-illuminated and dark images and are equally tagged

[1]The videos are located at *https://gofile.io/?c=iyfQND*.

as blurred in both low and high quality scenarios. Second, DCT metric fails to detect accurate blur levels, even if the image is blurred heavily i.e., it shows low blur differences (<0.2 blurriness) between high and low quality videos even though we created extremely low-quality videos (240p resolution and high (>200%) compression). Even for a single video, this DCT metric shows a lot of variation, such as for videos 3 and 11, raising concerns about its accuracy. We evaluate the accuracy of this blurriness metric in Section 6.4, showing a MOS error larger than 1.2. We also experiment with four other well-known blur metrics [15, 19, 21, 18], but none of these methods are consistent across diverse videos. This challenges the scalability and versatility of this blur metric in the wild.

The *temporal variation* metric proposed by Jana *et al* [16] aims to capture video stalls and considers the ratio of missed frames to total number of frames in a video, but the metric requires the number of frames sent over the network. We need the reference video to compute the total number of frames in the video, thus the metric is not entirely no-reference. In enterprise networks, a QoE metric needs to be applicable to diverse contents and to not rely on access to reference video. Further, there are many other previous works [32, 13, 22, 20] focused on measuring the temporal jerkiness. We find these methods either are parametrized or are sensitive to resolution and to frame rate of the video or are unable to scale across diverse video contents. The above limitations motivate us to propose new metrics that can accurately measure blurriness and freezes across diverse video content.

**Need for a model per application category:** When analyzing a recorded video for an application, the QoE metric has to be sensitive to the application category as different applications have to meet diverse performance guarantees. For instance, streaming quality is impacted largely by buffering and stall ratio, whereas telephony quality is impacted by bit rate, frames per second, blocking and blurring in the video. Table 2 lists examples of QoE metrics corresponding to different applications. Therefore, one needs to capture different artefacts when designing models for multiple application categories.

To address the aforementioned requirements, we seek to answer the question: *How to scalably label the quality of a video call, without any support from the application?*

| Application Category | Suitable Metric |
|---|---|
| Adaptive Streaming | Startup delay, Buffering ratio, Stall ratio |
| Video Telephony | Bitrate, Fps, Blocking, Blurring |
| Progressive Downloads | PSNR, SSIM |
| VR/AR, Game Streaming | Latency, buffering ratio, Stall ratio |

Table 2: Metrics based on application category

# 4. BACKGROUND

Before designing our no-reference QoE metrics, we present a video coding primer and QoE artefacts in video telephony. In Section 5, we harness these coding properties to carefully craft accurate metrics that capture such artefacts.

## 4.1 Video Coding Primer

Video coding is performed in three critical steps:

- **Frame prediction:** The encoder takes images of video and divides each image into macroblocks (typically 16x16, 16x8, 8x16, 8x8, 4x4 pixel blocks). The macroblocks are predicted from previously encoded macroblocks, either from current image (called *intra-frame prediction*) or from previous frames and future frames (called *inter-frame prediction*). Depending on the intra- and inter-macroblocks, frames are classified as I, P and B frames. The I frame uses only intra-frame prediction i.e., it does not employ any previously coded frames as reference. Whereas P frames are predicted using previously coded frames and B frames are encoded from previous and future frames. The encoder typically combines both intra- and inter-prediction techniques to exploit spatial and temporal redundancy, respectively. Intra-frame prediction involves different prediction modes [30] while finding candidate macroblocks. Inter-frame prediction uses motion estimation by employing different block matching algorithms (such as Hexagon based or full exhaustive search) to identify the candidate macroblock across frames. Finally, a residual is calculated by taking the difference (measured typically using mean absolute difference (MAD) or mean squared error (MSE)) between the predicted and current macroblock. The prediction stage produces 4x4 to 16x16 blocks of absolute-pixel or residual values.

- **Transform coding and quantization:** These absolute values are then transformed and quantized for further compression. Typically, two transform coding techniques (block or wavelet based) are used to convert pixel values into transform coefficients. A subset of these transform coefficients are sufficient to construct actual pixel values, which means reduced data upon quantization. The most popular transform coding is DCT over 8x8 macroblocks.

- **Entropy coding:** Finally, coefficients are converted to binary data which is further compressed using entropy coding techniques, such as CABAC, CAVLC or Huffman. Richardson presents details of video compression [30].

We highlight that inter-frame prediction depends on motion content in the video. The higher the motion in the video is, the lower the compression rate is. Similarly, intra-frame compression is affected by frame contents such as color variation. For instance, the blurrier the video is, the higher the compression rate is. In the next section, we design QoE metrics exploiting these video coding principles.

## 4.2 QoE Artefacts in Video Telephony

When a user is in a video telephony call, she can experience different aberrations in video quality, as follows.

**Video freeze** is a temporal disruption in a video. A user may experience freeze when the incoming video stalls abruptly and the same frame is displayed for a long duration. Additionally, freeze may appear as a fast play of video, where the decoder tries to recover from frame losses by playing contiguous frames in quick succession, creating a perception of `fast` movement. Both these temporal artefacts are grouped into freeze. This happens mainly due to network loss (where some frames or blocks lost) or delay (where the frames are dropped because the frames are decoded too late to display).

**Blurriness** appears when encoder uses high quantization parameters (QP) during transform coding. Typically, servers use adaptive encoding based on network conditions. In adaptive encoding, server attempts to adjust QP to minimize bi-

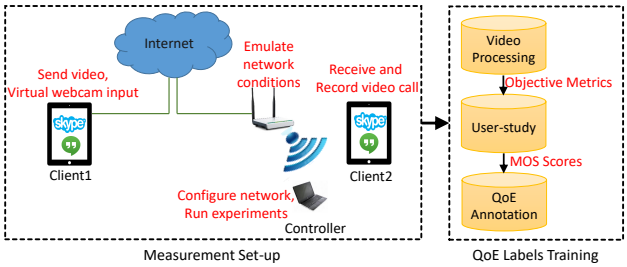


Figure 2: Measurement set-up and system architecture. *Left:* Video telephony measurements and recording video calls. *Right:* Our framework processing recorded videos offline and extracting objective metrics to predict QoE labels.

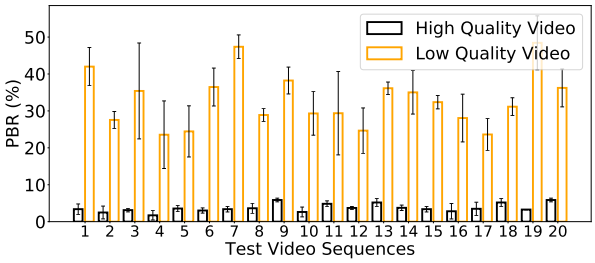


Figure 3: Blur detection using PBR.

trate in poor network conditions, which degrades the quality of encoded frame. High QP reduces the magnitude of high frequency DCT coefficients almost down to zero, consequently losing information and making it impossible to extract original DCT coefficients at the time of de-quantization. Loss of high-frequency information results in blurriness.

**Blocking:** Most of the current coding standards (such as H.26x and VPx) are block based, where each image is divided into blocks (from 4x4 to 32x32 and recent 64x64 block in H.265). The blocking metric captures the loss of these blocks due to high network-packet loss. The decoder can introduce visual impairments at the block boundaries or place random blocks in place of original blocks, if the presentation timestamp elapses, which creates bad experience.

**Call startup delay** is the duration of call setup from the time the caller initiates the call until the callee receives it. We observe an 11 s worst case and 7 s median delay when there is 20% network packet loss, whereas we obtain a median 3 s delay in best network conditions. Although call startup delay does measure user experience, it can only provide information at the beginning of the call, and not during the call.

In this work, we focus on freeze and blurriness artefacts. In our extensive experiments over Skype, Hangouts, FaceTime, we do not observe any blocking artefacts, hence we omit this metric for video telephony. We notice video freezes (temporal artefact) and blurring (spatial artefact). For video freezes, we explore multiple metrics that capture freeze ratio for whole clip, number of freezes per clip and duration of freezes. We do not consider startup delay, as it is an one-time metric.

# 5. DESIGN FOR SCALABLE QOE ANNOTATION

In this section, we first describe our framework and measurement methodology. We then explain our QoE metrics and evaluate them across different applications and devices. We validate that our metrics capture video artefacts caused by diverse network conditions.

## 5.1 Measurement Methodology

**Set-up:** In Figure 2, we show our measurement set-up and QoE labeling framework. Since video telephony is an interactive application, it requires at least two participating network end-points (clients). In our set-up, we use a mobile device on our local enterprise WiFi network (Client 1) and an Amazon-provided instance as the second end-point (Client 2). Both clients can run Skype or Hangouts[2]. When the video call is placed from Client 1 to Client 2, Client 2 runs a virtual web-cam that inputs a video file in telephony application instead of camera feed; at Client 1, the video is received during the call. At the Amazon Client 2, we use *manycam* [26], a virtual web-cam tool. This tool can be used with multiple video applications in parallel for automation. In our LAN, a controller sits to emulate diverse network conditions and to run experiments on the connected mobile device through Android debug bridge (ADB) interface (via USB or WiFi connection). To automate the video call process, we use AndroidViewClient (AVC) library [7]. Once the received call is accepted, we start the screen recording of the video call session. The videos are recorded using Az screen recorder [3]. The recorded videos are sent to video processing module to calculate the objective QoE metrics. We use Ffmpeg [2] tool to extract our QoE metrics. Ffmpeg is a video framework with large collection of coding libraries. To validate our metrics and translate them into user experience, the videos are then shown to users to rate their experience. Finally, we retrieve MOS from all users and map our QoE metrics to MOS. We delve into the details of our user study and modeling in Section 6.

**Network conditions:** As we experiment real-time with interactive applications (Skype, Hangouts, FaceTime), we need to emulate real user experience under any condition and to obtain samples with MOS values of all levels (1–5). Hence, we conduct tests with ideal network conditions and with throttled network. To create average and bad network conditions, we use Linux utility `tc` and we introduce hundreds of ms of delay, packet loss (10–20% ensuring that the call is setup), or low bandwidth (2–10 Mbps).

**Test video sequences:** We use the same 20 test video sequences as in Section 3. We collect these videos from Xiph media [27] and YouTube. We select 20 representative videos that contain different types of motion and content. All videos are downloaded in Full HD (1920x1280) resolution.

## 5.2 Our QoE Metrics

**PBR:** Video bitrate has been considered a standard metric for perceptual quality of video [23, **?**]. We compute the bitrate of recorded videos as a QoE metric. Typically, the bitrate is lower for low resolution video and higher for high resolution video and depends on the level of video compression. Therefore, we capture video blur with `encoded bitrate` by compressing the recorded video. We employ the observation that the blurrier the video is, the higher compression efficiency is. However, we find that the bitrate met-

[2]For FaceTime, we use 2 local clients (iPhone/iPad and MacBook Air) on different sub-networks, as creating virtual iOS and web-cam is challenging.

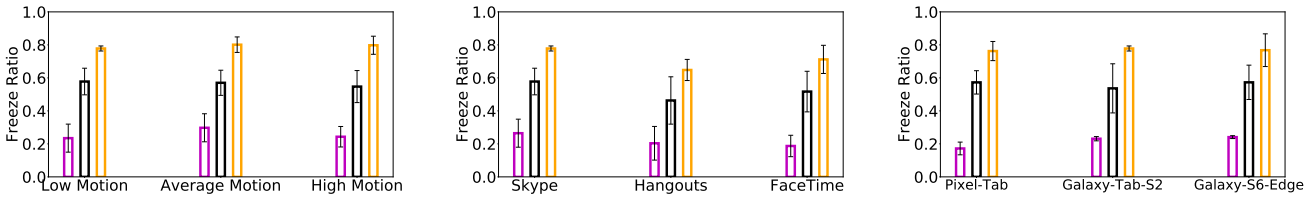


(a) Content and Motion (b) Applications (c) Devices

Figure 4: PBR and Freeze Ratio for different videos with respect to content, application and device settings. Results for diverse network conditions are shown (from bad, average, good).

ric is sensitive to motion in the video, because the block movement for high motion videos is very high and it is low for low motion videos. This results in different encoding bitrates. As described in Section 4, low motion videos take advantage of inter-frame prediction, which makes the encoded bitrate motion-sensitive. Therefore, we use intra-coded bitrate by *disabling the inter frame prediction while compressing video.* We experiment with different encoding parameters like quantization parameter (QP) and de-blocking filter techniques and we choose high QP value (30) while coding, to get large bitrate difference when encoding high- and low-quality videos. To achieve robustness to video content, we compute the *relative change between the recorded bitrate and the intra-coded bitrate of the compressed video.* We define this change as the perceptual bitrate (PBR), as it only captures quality of the image. Since we calculate PBR on the recorded video, we do not need a reference video, hence PBR is a no-reference metric.

We validate the PBR metric with respect to the same 20 videos used to compute blur using DCT coefficients in Section 3. We create two sets of videos with high and low quality and record them during a Skype call under best network conditions. This experiment aims to validate our blur capturing metric, hence we avoid video freezes by sending low quality videos over best network conditions. Fig. 3 shows PBR for both low and high quality videos. We observe a PBR larger than 20% for low quality videos, whereas PBR is smaller than 5% for high quality videos. Unlike blur detection using previous methods, we see a clean separation of average PBR between low and high quality videos. Therefore, PBR can be used to detect blurriness in videos without any ambiguity.

**Freeze Ratio:** As described in Section 4, freeze ratio is another important QoE artefact. Freeze ratio is the number of repeated frames over total frames in a given window, i.e., it denotes the amount of time the video is paused because of network disturbance. We use Ffmpeg's *mpdecimate* [2] filter in calculating freeze ratio. The *mpdecimate* algorithm works as follows: The filter divides the current and previous frame into 8x8 pixels blocks and computes sum of absolute differences (SAD) for each block. A set of thresholds (*hi, lo and frac*) are used to determine if the frames are duplicate. The thresholds *hi* and *lo* represent number of 8x8 pixel differences, so a threshold of 64 means 1 unit of difference for every pixel. A frame is considered to be duplicate frame if none of the 8x8 blocks yields SAD greater than a threshold of *hi*, and if no more than *frac* blocks have changed by more than *lo* threshold value. We experiment with several other error methods such as MSE and MAD, but we notice similar results among all three, thus we choose SAD for minimal computation overhead. We use threshold values of 64*12 for *hi*, 64*5 for *lo* and 0.1 for *frac* for all our experiments. The metric does not work if the entire video is having a still image (for instance a black screen throughout the video). However, we think that it is a reasonable assumption that most of video telephony applications do not generate such video content.

In addition to freeze ratio, we also compute length and number freezes in video. We define a freeze if the video is stalled for more than one second. We observe that users do not perceive the stall when the length of freeze is very short or if there are very few such short freezes in the video. Therefore, we employ `freeze ratio, length and number of freezes` metrics to capture the temporal artefacts of QoE.

## 5.3 Micro-Benchmarking of Video Artefacts

In this section, we show the scalability of our metrics through measurements across different applications and devices. As described above, we use a total of 4 metrics: PBR, freeze ratio, length and number of freezes in the video. For brevity, we show measurements for only PBR and freeze ratio. We find similar trends with other metrics as well. We measure these metrics with 6 different videos from the 20 videos described in Section 3, that cover high video-motion and content diversity. These experiments are run on Skype and Samsung Galaxy Tab S2 unless otherwise specified. All videos are recorded under Full HD (1920x1280) resolution with 60 Fps. Each experiment consists of 20 minutes video call with a total of 18 hours of video recordings. The videos are recorded under different network conditions to obtain different video quality levels. We use the following network conditions: good case (0% loss, 0 latency and 100 Mbps bandwidth), average case (5% loss, 100 ms and 1 Mbps bandwidth) and bad case (20% loss, 200 ms, and 512 Kbps bandwidth). Fig. 4 shows PBR and freeze ratio across different applications and devices. Our observations are the following.

**Video Motion and Content Diversity:** The average PBR for best network conditions is always smaller than 5%. PBR is larger than 20% under bad settings (see In Fig. **??**). The average freeze ratio for best network conditions is smaller than 0.3 and for bad conditions, it is larger than 0.8 (Fig. **??**). We observe that both PBR and freeze ratio are highly impacted by network conditions and follow same trend with network quality irrespective of content and motion in the video. Therefore, the videos can be labeled accurately because of clear separation between network dynamics.

**Application Diversity:** In Fig. **??**, **??**, we present PBR

and freeze ratio for three applications: Skype, FaceTime and Hangouts. For Skype, we observe an average PBR of less than 5% with good network and 20% with bad network. Whereas, both FaceTime and Hangouts reach more than 40% PBR under bad network. This discrepancy is due to application logic: Skype does not compromise quality of video, hence low PBR. But, this causes Skype video calls to be stalled more frequently compared to other applications under bad network scenarios. Whereas, bitrate adaptation of FaceTime and Hangouts sacrifices quality to provide temporally smooth video. Moreover, quality and bitrate are highly impacted by the underlying video codec the application uses. In our experiments, Skype uses H.264 whereas Hangouts uses VP8. We observe that using different video codecs and adaptive bitrate (ABR) algorithms impacts video quality during call.

The freeze ratio for Skype is similar to FaceTime and Hangouts. However, as network conditions worsen, Skype yields more freezes compared to other applications. Despite the additional freezes, the average freeze-ratio for Skype is only 0.1 larger than other applications. This is due to the longer freezes of FaceTime and Hangouts than of Skype.

**Device Diversity:** We aim to devise a model that is independent of the device that runs video telephony. Our metrics should capture similar video QoE on different devices given that screen recorder and network conditions are the same. To this end, we evaluate our metrics on three devices: Samsung Galaxy Tab S2, Samsung Galaxy Edge S6 and Google Pixel Tab. In Fig. **??**, **??**, we observe that both PBR and freeze ratio show same distribution under different network settings on all devices. Hence, our metrics are device independent.

# 6. FROM VIDEO ARTEFACTS TO QoE

We validate our QoE metrics presented in Section 5 with subjective measurements. We seek to ensure that our metrics accurately capture video telephony QoE artefacts. Video artefacts vary across applications and network conditions. Additionally, they can appear together (e.g., when we have both blurriness and stutter) or independently. Intermingled video artefacts result in diverse QoE levels (from bad to excellent), standardized as MOS by ITU-T [31][3]. We carry out a user study and obtain a MOS for each video.

## 6.1 Data Preparation

As described in Section 5, the dataset is prepared from recorded video calls. We use 20 videos described in Section 3, for video calls on Skype, FaceTime and Hangouts. For each video and application, we repeat experiments on multiple devices. The video calls are recorded under different network conditions to produce good, average and bad quality videos. We record video calls for Skype, Hangouts on Samsung Galaxy (SG) S6 edge, Google Pixel Tab, SG S2 Tab and for FaceTime on iPad Pro (model A1674) and iPhone 8 Plus. We post-process these videos into 30 seconds video clips and evaluate QoE for each clip. We host a web server with these video clips and ask the users to rate their experience after watching each sample.

## 6.2 User-Study Setup

We conduct the user-study in two phases: 1) in two labs, 2) online using a crowd sourced platform. The lab user study is conducted at a university campus and an enterprise lab. The online user study is conducted on Amazon Mechanical Turk platform [1]. Online users are from the United States and are in age range 20–40. We collect results from 60 lab users and more than 150 online users[4]. We faced several challenges while deploying a user-study in the wild, such as ensuring that 1) users watch the whole video clip without fast forwarding and then rate their experience, 2) users can rate the video if and only if they watch the video, 3) users watch on screens of similar size to avoid huge QoE variance i.e., small screen users do not perceive poor quality compared to large screen users. We address these challenges by carefully designing the user-study website and avoiding noisy samples. First, we disable the video controls in the web page so that users cannot advance the video. Second, we introduce random attention pop-up buttons while watching the video and ask users to click on the attention button to confirm that they are watching the video. A user cannot move to next video until the current video is rated. Finally, we restrict users from taking the study on mobile devices, to avoid variance due to small screens. The user-study web page can be run on Chrome, Firefox and Safari. Once the user completes rating all the videos, results are pushed to our server. Then, users are granted a server-generated code for processing payments in MTurk. Amazon MTurk restricts users from taking again the same study, thus our users are unique.

## 6.3 Lab vs. MTurk Users

We compare the MOS across lab and online users for the same set of 40 video clips and we find similar distributions across 80 clips. Fig. 5 shows the MOS bar plots of user ratings. The lower the rating is, the lower the QoE is. For each video sequence, we plot the average MOS across users with error bars for standard deviation. We observe that lab and online users exhibit similar distributions of MOS. The standard deviation of MOS between lab and online users is smaller than 1 MOS for 96% of videos. We find that 4% of these video clips have more than 1 MOS standard deviation and we remove them from our analysis as outliers. Such videos have a large portion of uniform background, hence their content challenges classification between average and good MOS.

## 6.4 Modeling Our Metrics to MOS

We now present our MOS prediction model that corroborates that our metrics accurately capture QoE artefacts and users' MOS. We build a model to map our objective metrics to subjective evaluations (MOS from user-study). Typically network administrators need to estimate a subjective evaluation such as MOS. However, QoE assignment in 5 classes can be cumbersome and may give little information on network quality. Hence, we map MOS scores to 3 classes (i.e., bad, average, good) that can be used by LTE or WiFi deployments to enhance resource allocation. We first explain our modeling methodology from freeze and blur metrics to MOS, and then describe how to translate MOS into 3-class QoE.

[3]MOS takes values from 1 to 5, with 5 being excellent.

[4]Our conducted user-studies are approved by the Institutional Review Board (IRB) of our institution. Evidence to be provided upon paper acceptance.

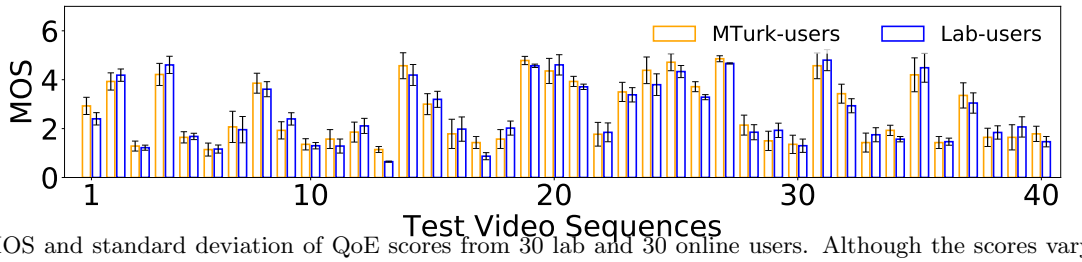

Figure 5: MOS and standard deviation of QoE scores from 30 lab and 30 online users. Although the scores vary across the users both in lab and online, the distribution of MOS is similar in two cases.

Typically, objective QoE metrics are mapped to MOS scores using non-linear regression [9]. Our regression model employs the average MOS from 15 users as ground-truth per video clip and it is based on ensemble methods [28]. Taking the ensemble of models, we combine predictions of base estimators to improve generalizability and robustness over a single model. Moreover, a single model is always vulnerable to over-fitting and is complicated, which can be avoided in the form of ensemble of weak models. The ensemble is usually produced by two methods: *averaging* or *boosting*. We employ boosting method, in particular `AdaBoost`[25], where the base estimators are built sequentially and one tries to reduce the bias of the combined estimator, thereby combining several weaker models and producing an accurate model.

`AdaBoost` algorithm fits a sequence of weak models (for example, small decision trees in our framework nearly equivalent to random guessing) on different versions of data. The predictions from each weak model are combined to produce a strong prediction with a weighted sum scheme. At each iteration, called boosting iteration, a set of weights $(w_1, w_2, , w_N$, where $N$ is number of samples) are applied to training data. The weights are initialized with $w_i = 1/N$, in order to train a weak model on the original data. In the following iterations, the weights of training samples are individually modified and model is applied again on the re-weighted data. At any given boosting stage, the weights are changed depending on prediction at the previous step. The weights are proportionately increased for incorrectly predicted training samples, while the weights are decreased for those samples that were correctly predicted. The samples which are difficult to predict become more important as the number of iterations increases. The next-iteration weak model then focuses on the incorrectly predicted samples in the previous step. Details of the Adaboost algorithm are given in [25][10].

Moving from 5 MOS scores to 3 classes, one has to estimate two thresholds $m_1, m_2$ in MOS (bad label: MOS $< m_1$, average: $m_1 \leq$ MOS $< m_2$, good: MOS $\geq m_2$). To this end, we first train the regression model and then search the MOS scores space with a sliding window of 0.05 for the two thresholds. We iterate over all such possible thresholds to maximize the accuracy of the trained model. We compute the true labels and prediction labels from the test MOS scores and predicted scores respectively using the corresponding thresholds in each iteration. We then select the thresholds which give highest accuracy from prediction labels. Therefore, our framework is divided into two phases: predicting MOS scores and labeling the scores with optimal thresholds.

We first evaluate our metrics by fitting five most common regressors: Support Vector Regressor (SVR), Random Forests (RF), Multi-Layer Perceptron (MLP), K-Nearest Neighbor (KNN) and Adaboosted Decision Tree Regressors (ADT).

Table 3: Models performance on Skype data

| Model | Precision (%) | Accuracy (%) | Recall (%) | MSE |
|---|---|---|---|---|
| SVR | 89.33 | 89.33 | 89.33 | 0.36 |
| MLP | 90.77 | 90.77 | 89.62 | 0.36 |
| KNN | 82.91 | 81.67 | 81.67 | 0.63 |
| RF | 89.72 | 89.34 | 89.34 | 0.41 |
| ADT | 92.21 | 92.00 | 92.00 | 0.29 |

Table 4: Models performance on FaceTime data

| Model | Precision (%) | Accuracy (%) | Recall (%) | MSE |
|---|---|---|---|---|
| SVR | 88.13 | 86.00 | 86.00 | 0.32 |
| MLP | 90.00 | 89.77 | 89.30 | 0.28 |
| KNN | 74.98 | 72.00 | 72.30 | 0.48 |
| RF | 90.37 | 90.00 | 90.00 | 0.28 |
| ADT | 90.28 | 90.00 | 90.00 | 0.26 |

Each model is evaluated under 10 fold cross-validation. We perform a fine grid search to tune the hyper-parameters for all the models. We select the best parameters from the grid search and use the best estimator for the rest of the evaluations. This is repeated for Skype, FaceTime and Hangouts applications separately. The performance of each model is presented in terms of precision, accuracy and recall for three applications after labeling stage. We present micro-average metrics of accuracy, precision and recall, as the macro-average does not yield class importance [4]. Micro-average aggregates the contributions from all the classes to compute the average metric. We also report the mean squared error (MSE) for all models. We observe at least 88% accuracy for all the models in all applications, except KNN regressor. This discrepancy is due to the weakness of KNN with multiple features. We observe that KNN does not generalize our dataset well and predicts most of the samples incorrectly. The mis-prediction is due the fact that each sample in higher dimension is an outlier as the distance metric (euclidean distance in our model) becomes weak with more features [29], unless the data is well separated in all dimensions. Among all models, ADT has consistent and better accuracy in all applications with a maximum accuracy of 92% in Skype, 90% in FaceTime and 93.33% in Hangouts. We also use boosting with other models, but boosting did not improve the accuracy. Therefore, as ADT performs better than other models, we use this model for all the other evaluations unless otherwise specified. The best hyper-parameters for ADT from grid search are: `n_estimators = 10, learning_rate = 0.1` and `linear` loss [28].

Fig. 6 shows a scatter plot of user-study MOS vs. predicted MOS for the three applications. The MSE in MOS for the three applications is smaller than 0.4 with ADT for all the applications. We also observe three clear clusters approximately divided by the MOS scores $m_1 = 2$ and $m_2 = 4$, that coincide with our thresholds for labeling the scores into 3 classes. This also justifies our design choice to finally em-

Table 5: Models performance on Hangouts data

| **Model** | **Precision (%)** | **Accuracy (%)** | **Recall (%)** | **MSE** |
|---|---|---|---|---|
| SVR | 91.36 | 90.67 | 90.67 | 0.44 |
| MLP | 89.34 | 88.48 | 88.48 | 0.45 |
| KNN | 87.02 | 86.67 | 86.67 | 0.49 |
| RF | 91.22 | 90.67 | 90.67 | 0.43 |
| ADT | 93.75 | 93.33 | 93.33 | 0.38 |

Table 6: Model performance across devices for Skype

| Devices | | Model Performance | | |
|---|---|---|---|---|
| Training | Testing | Precision (%) | Accuracy (%) | Recall (%) |
| SG-S6 Phone | SG-S6 Phone | 89.90 | 88.57 | 88.57 |
| | SG-S2 Tab | 88.41 | 88.00 | 88.00 |
| | Pixel Tab | 88.52 | 87.62 | 87.62 |
| SG-S2 Tab | SG-S6 Phone | 83.73 | 84.43 | 83.00 |
| | SG-S2 Tab | 93.04 | 91.43 | 91.43 |
| | Pixel Tab | 82.69 | 82.86 | 82.86 |
| Pixel Tab | SG-S6 Phone | 84.43 | 84.00 | 84.00 |
| | SG-S2 Tab | 84.40 | 86.49 | 86.49 |
| | Pixel Tab | 88.20 | 94.40 | 94.00 |

ploy three labels (bad, average, good) out of 5 MOS scores.
**Model performance for Skype:** Table 3 shows performance of Skype model across different regressors. The MSE in MOS is 0.29 in case of ADT and it is 0.63 with KNN regressor. Similarly, precision, accuracy and recall for ADT is the highest, while KNN being lowest. ADT model gives a best threshold of $m_1 = 2$ and $m_2 = 3.8$ in separating the MOS scores into labels. While all the other models produce a threshold of $m_1 = 2$ and $m_2 = 3.4$. Here, the best performance in ADT results from $(i)$ its low MSE and $(ii)$ the wide range for average class separation, i.e., it labels all the samples from MOS 2 to 3.8 as average class, while other models yield average class from MOS 2 to 3.4. The performance gap is due to the distribution of our average class samples spread over wider range of bad or good labels. Using $m_1 = 2$ and $m_2 = 3.8$ thresholds, we get 30%, 40% and 30% of our 300 samples in bad, average and good labels.

To show that our Skype model is device independent, we further evaluate our model across three devices: SG-S6 phone, SG-S2 Tab and Pixel Tab. Table 6 shows precision, accuracy and recall for all three devices. We measure performance by training on one device, and testing on other devices. We observe that the performance is always better when trained and tested on the same device compared to training on one device and testing on other device. However, we find a difference of less than 7% in accuracy when trained and tested across different devices, with an accuracy of at least 83%. This corroborates that our model is robust across devices and it can be trained and tested without device constraints i.e., our metrics can collected on a certain device and can be applied to any other devices for Skype.
**Model performance for FaceTime:** Table 4 shows performance of FaceTime model across different regressors. Similar to Skype, we observe similar performance (> 89% accuracy) for all models except the KNN regressor. Here, although the RF regressor is performing better (90.37% precision) than ADT, the MSE in MOS is larger than ADT. Interestingly, all models produce same thresholds of $m_1 = 2$ and $m_2 = 3.4$ in labeling the scores. Here, the samples are distributed uniformly across three classes unlike Skype, hence all regressors are performing almost equally. However, KNN regressor still suffers in FaceTime model due to weakness with many features as explained above. Using these thresholds, we get 30%, 36% and 34% of the 200 samples in bad, average and good labels.

Table 7: Model performance across devices for FaceTime

| Devices | | Model Performance | | |
|---|---|---|---|---|
| Training | Testing | Precision (%) | Accuracy (%) | Recall (%) |
| iPad Pro | iPad Pro | 93.60 | 92.00 | 92.00 |
| | iPhone 8 Plus | 90.18 | 89.93 | 89.93 |
| iPhone 8 Plus | iPad Pro | 88.34 | 88.34 | 88.34 |
| | iPhone 8 Plus | 92.50 | 92.00 | 92.00 |

Table 8: Model performance across devices for Hangouts

| Devices | | Model Performance | | |
|---|---|---|---|---|
| Training | Testing | Precision (%) | Accuracy (%) | Recall (%) |
| SG-S6 Phone | SG-S6 Phone | 90.03 | 90.00 | 90.00 |
| | SG-S2 Tab | 84.26 | 84.77 | 84.77 |
| | Pixel Tab | 82.86 | 82.00 | 82.00 |
| SG-S2 Tab | SG-S6 Phone | 89.61 | 89.21 | 89.21 |
| | SG-S2 Tab | 91.76 | 90.00 | 90.00 |
| | Pixel Tab | 85.41 | 84.77 | 84.77 |
| Pixel Tab | SG-S6 Phone | 86.79 | 86.00 | 86.00 |
| | SG-S2 Tab | 85.05 | 85.00 | 85.00 |
| | Pixel Tab | 86.17 | 86.67 | 86.67 |

To validate that our FaceTime model is device independent, we train and test across iPad and iPhone devices. Table 7 shows that when training and testing on same device, we observe 92% accuracy. Whereas, training and testing across devices yields at least 88% accuracy. Hence, we observe a difference of 4% accuracy across device training and testing. Our FaceTime model is also device-independent. Note that, we are not comparing the performance of our model training on Android devices and testing on iOS devices and vice-versa, because the recording set-up is different these environments.
**Model performance for Hangouts:** Table 5 shows performance of Hangouts model across different regressors. Similar to other applications, ADT outperforms other models with 93.33% accuracy with an average MSE of 0.38. Similar to FaceTime, we observe that all models produce same thresholds of $m_1 = 2$ and $m_2 = 3.5$ in labeling the scores. Using the above thresholds, we get 32%, 34% and 34% of the 300 samples in bad, average and good labels respectively.

We further evaluate the Hangouts model across three devices: SG-S6 phone, SG-S2 Tab and Pixel Tab. Table 8 shows that an accuracy of at least 86.67% when training and testing on same device, while inter-device train and test gives an accuracy of at least 82%. Overall, we observe less than 8% accuracy difference when trained and tested across different devices. This shows that the model is independent of where training and tested are conducted.

## 6.5 Comparison with Baseline and Feature Importance

We compare our model prediction error with previous work for Skype application. As we need no-reference metrics for the baseline comparison, we use the DCT blur metric used by Jana *et al* as spatial metric and frame-drop metric in [22] as temporal metric. We fit the ADT model with these two metrics as well as with our metrics using the MOS scores from our user-study. Fig. 7 shows the performance of Skype application across the 20 videos described in Section 3. Clearly, for a single video, both baseline and our model yield less than 0.2 MSE in MOS whereas as the number of videos increases, the MSE grows larger than 1.3 MOS for baseline metrics. Whereas, our model has a maximum of 0.4 MSE. The baseline metric's high MOS error with large

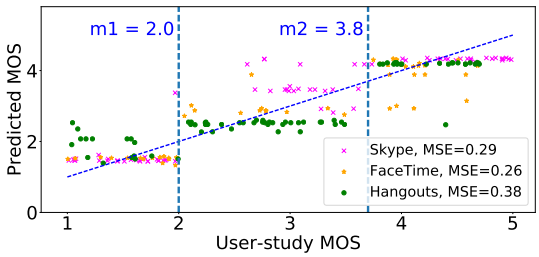


Figure 6: User-study vs. predicted MOS for the three applications. We also show 3 clear QoE clusters divided by our thresholds $m_1 = 2$ and $m_2 \approx 3.8$.

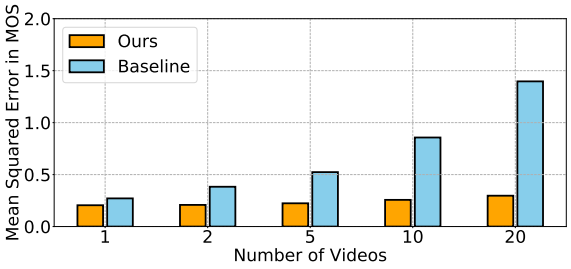


Figure 7: Comparison of our metrics vs. baseline. Baseline has an up to 1.4 MOS estimation error across 20 video contents, hence failing to distinguish good/bad from average QoE.

number of videos is due to DCT metric's inability to scale across diverse video content. In fact, in our experiments we measure feature importance, which is defined as the amount each feature improves performance weighted by the number of samples this feature is responsible for. We observe that feature importance for DCT is as low as 0.1, and it is 0.9 for frame-drop metric. Therefore, previous metrics fail to model video telephony QoE across diverse videos. We observe similar results for FaceTime and Hangouts.

We also evaluate the importance of each proposed metric. Fig. 8 shows the importance of features for ADT over all three applications. Out of all features, freeze ratio is dominating with at least 0.5 feature importance on all applications. For Skype, we observe highest ($> 0.7$) importance to freeze ratio. The rest of the metrics are almost equally important, and removal of any of these features causes an up to 0.2 accuracy degradation. Whereas, for FaceTime and Hangouts, we notice high importance for PBR (0.28 for FaceTime and 0.41 for Hangouts) due to their compromise in quality over freezes.

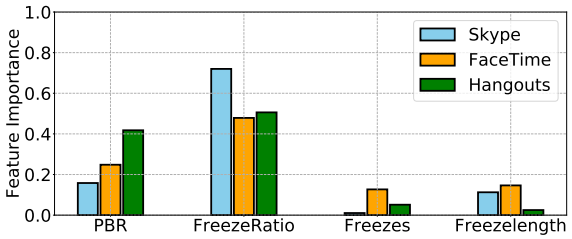


Figure 8: Feature Importance for the three applications.

## 7. CONCLUSION

## 8. REFERENCES


[1] Amazon Mechanical Turk. https://www.mturk.com/.

[2] FFmpeg. ffmpeg.org/.

[3] http://az-screen-recorder.en.uptodown.com/android.

[4] Micro- vs. Macro-Average. https://www.clips.uantwerpen.be/ vincent/pdf/microaverage.pdf.

[5] Space Pirate Trainer. www.spacepiratetrainer.com/.

[6] theBlu: Encounter. wevr.com/project/theblu-encounter.

[7] Android View Cient (AVC). https://github.com/dtmilano/androidviewclient.

[8] Kuan-Ta Chen, Chun-Ying Huang, Polly Huang, and Chin-Laung Lei. Quantifying skype user satisfaction. In *ACM SIGCOMM*, 2006.

[9] Li Cui and Alastair R Allen. An image quality metric based on corner, edge and symmetry maps. In *BMVC*, pages 1–10, 2008.

[10] Harris Drucker. Improving regressors using boosting techniques. In *ICML*, 1997.

[11] Aggarwal et.al. Prometheus: toward quality-of-experience estimation for mobile apps from passive network measurements. In *ACM HotMobile*, 2014.

[12] Balachandran et.al. Developing a predictive model of quality of experience for internet video. In *ACM SIGCOMM*, 2013.

[13] Borer et.al. A model of jerkiness for temporal impairments in video transmission. In *IEEE QoMEX*, 2010.

[14] Fiedler et.al. A generic quantitative relationship between quality of experience and quality of service. *IEEE Network*, 24(2), 2010.

[15] Golestaneh et.al. No-reference quality assessment of jpeg images via a quality relevance map. *IEEE signal processing letters*, 21(2):155–158, 2014.

[16] Jana et.al. Qoe prediction model for mobile video telephony. *Multimedia Tools and Applications*, 75(13):7957–7980, 2016.

[17] Marichal et.al. Blur determination in the compressed domain using dct information. In *IEEE ICIP*, 1999.

[18] Marziliano et.al. A no-reference perceptual blur metric. In *IEEE ICIP*, 2002.

[19] Mittal et.al. No-reference image quality assessment in the spatial domain. *IEEE Transactions on Image Processing*, pages 4695–4708, 2012.

[20] Pastrana-Vidal et.al. Automatic quality assessment of video fluidity impairments using a no-reference metric. In *VPQM*, 2006.

[21] Tong et.al. Blur detection for digital images using wavelet transform. In *IEEE ICME*, 2004.

[22] Usman et.al. A no reference video quality metric based on jerkiness estimation focusing on multiple frame freezing in video streaming. *IETE Technical Review*, 34(3):309–320, 2017.

[23] Zhang et.al. Profiling skype video calls: Rate control and video quality. In *IEEE INFOCOM*, 2012.

[24] Cisco VNI Forecast. Cisco visual networking index: Global mobile data traffic forecast update, 2016–2021 white paper. 2017.

[25] Yoav Freund and Robert E Schapire. A decision-theoretic generalization of on-line learning and an application to boosting. *Journal of computer and system sciences*, 55(1):119–139, 1997.

[26] Manycam. https://manycam.com/.

[27] media.xiph.org/video/derf/. Xiph.org Video Test Media.

[28] Ensemble Methods. http://scikit-learn.org/stable/modules/ensemble.html.

[29] Vladimir Pestov. Is the k-nn classifier in high dimensions affected by the curse of dimensionality? *Computers & Mathematics with Applications*, 65(10):1427–1437, 2013.

[30] Iain E Richardson. *H. 264 and MPEG-4 video compression: video coding for next-generation multimedia*. John Wiley & Sons, 2004.

[31] BT Series. Methodology for the subjective assessment of the quality of television pictures. *Recommendation ITU-R BT*, pages 500–13, 2012.

[32] Stephen Wolf and M Pinson. A no reference (nr) and reduced reference (rr) metric for detecting dropped video frames. In *VPQM*, 2009.